

Extrinsic Information Transfer Functions: A Model and Two Properties

A. Ashikhmin, G. Kramer, S. ten Brink
Lucent Technologies, Bell Labs
600 Mountain Ave, Murray Hill NJ 07974, U.S.A.
e-mail: {aea,gkr,stenbrink}@bell-labs.com.

Abstract — Extrinsic information transfer (EXIT) charts are a tool for predicting the convergence behavior of iterative decoding of concatenated codes. The EXIT analysis is made precise by introducing a model of the decoding process and specifying the desired information-theoretic quantities. The model applies to iterative decoding of parallel concatenated, serially concatenated, and low-density parity-check codes. Furthermore, the model leads to a duality property and an area property of EXIT charts. The latter property suggests that it is advantageous to use a rate-one inner code when iteratively decoding serially concatenated codes.

I. INTRODUCTION

Extrinsic information transfer (EXIT) charts predict the convergence behavior of iterative decoding and detection schemes [1]. Experience suggests the charts are accurate, but there is a lack of proofs explaining why they work. The main purpose of this paper is twofold: first, to introduce a model for analyzing EXIT charts, and second, to prove properties of EXIT charts that explain some of the observations that have been made by simulations.

We consider the following example of an EXIT chart to demonstrate the use of the tool. Suppose we transmit a message using a low-density parity-check (LDPC) code [2, 3]. Such a code is often represented by a bipartite graph whose left vertices are called *variable* nodes and whose right vertices are called *check* nodes [4, 5]. Suppose the variable and check nodes have degree 2 and 4, respectively, so that we have a (2,4)-regular LDPC code. The code has a design rate of 1/2 and, as is usually done, we assume the code is long and its interleaver has large girth.

Suppose we transmit the code words over a binary erasure channel (BEC) with erasure probability q . The reason for studying the BEC is because a belief-propagation decoder passes only one of three probabilities: 0, 1 and 1/2 (erasure). As a consequence the EXIT functions can be computed exactly and, in fact, the transfer functions are one minus the fraction of erasures being passed from one side of the graph to the other. Hence the BEC EXIT analysis reduces to that of [4]. Fig. 1 shows the EXIT functions when $q = 0.3$ and $q = 0.5$. The curve for the check nodes is the one starting at 0 on the I_A^c axis, and its functional form is $I_E^c = (I_A^c)^3$. The curve for the variable nodes depends on q and is given by $I_E^v = 1 - q \cdot (1 - I_A^v)$.

The decoding trajectories are depicted in Fig. 1 by the dashed lines marked with arrows. For instance, when $q = 0.3$ we begin on the I_A^c axis at $1 - q = 0.7$ and move right to the check node curve. We then move up to the variable node

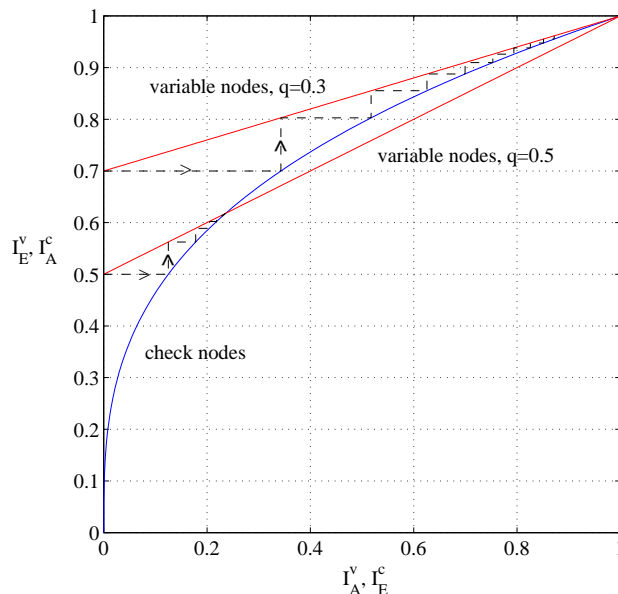


Fig. 1: EXIT functions for a (2,4)-regular LDPC code on the BEC with erasure probabilities $q = 0.3$ and $q = 0.5$.

curve marked $q = 0.3$, back to the check node curve, and so forth. It turns out that the curve marked $q = 0.3$ does *not* intersect the check node curve. This means the decoder's per-edge erasure probability can be made to approach zero. In contrast, the curve marked $q = 0.5$ intersects the check node curve – this means the decoder will get “stuck”. In fact, one can show the variable node curve intersects the check node curve if $q \geq 1/3$ and does not intersect it otherwise. The erasure probability $q = 1/3$ is therefore a *threshold* for the decoder. Observe that the code design rate is 1/2 while the capacity of a BEC with erasure probability 1/3 is 2/3. Thus, (2,4)-regular LDPC codes do not approach capacity with iterative decoding. We remark that it is known that *irregular* LDPC codes can approach capacity on the BEC [4].

Suppose next that we transmit the code words over a discrete memoryless channel (DMC) that is not the BEC. Now an exact analysis of the belief-propagation decoder can be difficult because the probabilities being propagated take on a growing number of values with the number of iterations. One technique for analyzing such cases is to use *density evolution* [5]. A second technique is to use EXIT charts, and it is this approach we consider here.

This paper is organized as follows. In Section II we describe the model and derive certain information-theoretic quantities. The model can be used for any DMC. Section III gives two properties of EXIT charts when the *a priori* information is modeled as coming from a BEC. The second property relates

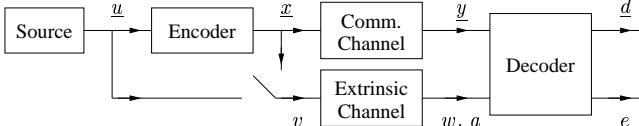


Fig. 2: The basic decoding model.

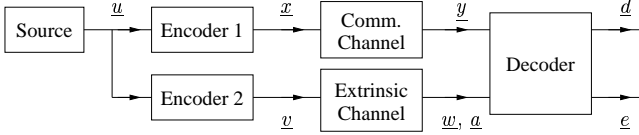


Fig. 3: A general decoding model.

the area under an EXIT curve to certain entropies. Sections IV and V show how the area property can help guide the design of serially concatenated and LDPC codes.

II. MODEL AND EXTRINSIC INFORMATION

A. DECODING MODEL

The basic decoding model is shown in Fig. 2. A binary symmetric source produces a vector \underline{u} of k independent information bits each taking on the values 0 and 1 with probability $1/2$. A rate k/n encoder maps \underline{u} to a binary length- n code word \underline{x} . The decoder receives two vectors: a noisy version \underline{y} of \underline{x} and a noisy version \underline{w} of \underline{v} , where \underline{v} is either \underline{u} or \underline{x} . We call the \underline{x} to \underline{y} channel the *communication channel*, and the \underline{v} to \underline{w} channel the *extrinsic channel*. The latter name emphasizes that \underline{w} originates from outside the communication channel [6]. Usually both channels are memoryless, although some of our results remain valid when the communication channel has memory.

The model of Fig. 2 might seem unusual to the reader who is used to seeing *a priori* information enter the decoder as independent information from a second source. In fact, this *a priori* information is represented by \underline{w} . We prefer to consider \underline{w} as the output of a channel because this makes the relation between \underline{w} and \underline{u} explicit.

A somewhat more general model than that of Fig. 2 is shown in Fig. 3. To see that Fig. 3 includes Fig. 2 as a special case, let Encoder 1 be the Encoder in Fig. 2. Then if $\underline{v} = \underline{u}$ we make Encoder 2 the identity mapping, and if $\underline{v} = \underline{x}$ Encoder 2 is simply Encoder 1. However, when dealing with LDPC codes we will make Encoder 1 the identity mapping and Encoder 2 a repeat code or parity-check code. This situation is not included in Fig. 2.

We continue by considering Fig. 3. Let m be the length of \underline{v} . The decoder uses \underline{y} and \underline{w} to compute two estimates of \underline{v} : the *a posteriori* values \underline{d} and the *extrinsic* values \underline{e} . We interpret the symbol w_j as giving *a priori* information about the random variable V_j with log-likelihood-ratio

$$a_j = \log \frac{P(w_j | V_j = 0)}{P(w_j | V_j = 1)}. \quad (1)$$

The decoder we are mainly interested in is the maximum *a posteriori* (MAP) bit decoder [7] that computes the soft output log-likelihood-ratio

$$d_j = \log \frac{\Pr(V_j = 0 | \underline{y}, \underline{w})}{\Pr(V_j = 1 | \underline{y}, \underline{w})} \quad (2)$$

for all j . For convenience, we write $\underline{v}_{[j]}$ for the vector \underline{v} with the j th term removed, i.e., $\underline{v}_{[j]} = [v_1, \dots, v_{j-1}, v_{j+1}, \dots, v_m]$. We expand the numerator in (2) as

$$\begin{aligned} \Pr(V_j = 0 | \underline{y}, \underline{w}) &= \sum_{\underline{u}: v_j(\underline{u})=0} P(\underline{u} | \underline{y}, \underline{w}) \\ &= \sum_{\underline{u}: v_j(\underline{u})=0} \frac{P(\underline{u})P(\underline{w} | \underline{u})P(\underline{y} | \underline{u}, \underline{w})}{P(\underline{y}, \underline{w})} \\ &= \sum_{\underline{u}: v_j(\underline{u})=0} \frac{P(\underline{u})P(\underline{w} | \underline{v}(\underline{u}))P(\underline{y} | \underline{x}(\underline{u}))}{P(\underline{y}, \underline{w})} \\ &= \frac{P(w_j | V_j = 0)}{P(\underline{y}, \underline{w})} \sum_{\underline{u}: v_j(\underline{u})=0} P(\underline{u}) \\ &\quad P(\underline{w}_{[j]} | \underline{v}_{[j]}(\underline{u}))P(\underline{y} | \underline{x}(\underline{u})), \end{aligned} \quad (3)$$

where $\underline{v}(\underline{u})$ and $\underline{x}(\underline{u})$ are vectors corresponding to \underline{u} , and where the last step follows because the extrinsic channel is memoryless. Expanding the denominator of (2) in the same way and inserting the result into (2), we have

$$\begin{aligned} d_j &= \log \frac{\Pr(w_j | V_j = 0)}{\Pr(w_j | V_j = 1)} \\ &\quad + \log \frac{\sum_{\underline{u}: v_j(\underline{u})=0} P(\underline{w}_{[j]} | \underline{v}_{[j]}(\underline{u}))P(\underline{y} | \underline{x}(\underline{u}))}{\sum_{\underline{u}: v_j(\underline{u})=1} P(\underline{w}_{[j]} | \underline{v}_{[j]}(\underline{u}))P(\underline{y} | \underline{x}(\underline{u}))} \\ &= a_j + e_j, \end{aligned} \quad (4)$$

where e_j is the *extrinsic value* about v_j defined as the second term on the right side of (4). We will consider e_j as a realization of the random variable E_j .

It turns out that for iterative decoding of *parallel concatenated codes* we must define e_j differently than above if u_j is transmitted as a *systematic bit* x_ℓ . For such positions j we must use

$$e_j = \log \frac{\sum_{\underline{u}: v_j(\underline{u})=0} P(\underline{w}_{[j]} | \underline{v}_{[j]}(\underline{u}))P(\underline{y}_{[\ell]} | \underline{x}_{[\ell]}(\underline{u}))}{\sum_{\underline{u}: v_j(\underline{u})=1} P(\underline{w}_{[j]} | \underline{v}_{[j]}(\underline{u}))P(\underline{y}_{[\ell]} | \underline{x}_{[\ell]}(\underline{u}))}, \quad (6)$$

where we have removed $c_j = \log[P(y_\ell | u_j = 0)/P(y_\ell | u_j = 1)]$ from the e_j of (5). Thus, we now have

$$d_j = a_j + c_j + e_j. \quad (7)$$

B. EXIT CHARTS

An iterative decoding scheme usually has two decoders that pass their extrinsic values to each other. More precisely, the e_j from one decoder pass through an interleaver and are fed to the other decoder as *a priori* values \underline{a} . We model \underline{a} as being output from a memoryless channel as in Fig. 3. The EXIT chart will depict how much each decoder “amplifies” the knowledge about the v_j as measured from the decoder inputs a_j to the decoder outputs e_j .

We begin with the information transfer from the v_j to the e_j . For this we compute the average of the mutual informations $I(V_j; E_j)$ across the decoder, i.e.,

$$I_E := \frac{1}{m} \sum_{j=1}^m I(V_j; E_j). \quad (8)$$

The value I_E is called the *average extrinsic information* out of the decoder. Consider first the e_j of (5). Observe from (4)

that e_j is a function of \underline{y} and $\underline{w}_{[j]}$, and that $\underline{w}_{[j]}$ and $\underline{a}_{[j]}$ are interchangeable since one defines the other. The combination of these two results means that

$$I(V_j; E_j) \leq I(V_j; \underline{Y} \underline{W}_{[j]}) = I(V_j; \underline{Y} \underline{A}_{[j]}). \quad (9)$$

The following proposition shows that the inequality in (9) is in fact an equality.

Proposition 1 For e_j defined as in (4) and (5) we have

$$I(V_j; E_j) = I(V_j; \underline{Y} \underline{A}_{[j]}). \quad (10)$$

Using this proposition, we can write

$$I_E = \frac{1}{m} \sum_{j=1}^m I(V_j; \underline{Y} \underline{A}_{[j]}). \quad (11)$$

We remark that for non-MAP bit decoders the ‘‘extrinsic information’’ put out by the decoder will usually not satisfy (9) with equality.

Next, consider the usual parallel concatenated code for which *all* the u_j are transmitted as systematic bits and $\underline{v} = \underline{u}$. For such codes we must use the e_j of (5) for *all* j . For simplicity, let \underline{u} be the first k bits of \underline{x} so e_j is a function of $\underline{y}_{[j]}$ and $\underline{a}_{[j]}$. Furthermore, as in Proposition 1 one can show that $I(V_j; E_j) = I(V_j; \underline{Y}_{[j]} \underline{A}_{[j]})$ so (8) becomes

$$I_E = \frac{1}{m} \sum_{j=1}^m I(V_j; \underline{Y}_{[j]} \underline{A}_{[j]}). \quad (12)$$

In the sequel we shall consider only the definition (11) to avoid writing everything twice. The extensions to parallel concatenated codes with systematic bits follow from the other derivations.

Consider now the information transfer from the v_j to the a_j . For this we compute the *average a priori information* defined as

$$I_A := \frac{1}{m} \sum_{j=1}^m I(V_j; A_j) = I(V_1; A_1), \quad (13)$$

where the second step follows because all the V_j are assumed to have the same distribution. An EXIT chart plots I_E as a function of I_A . Again, the idea is that this transfer function quantifies how well the decoder improves the knowledge about the v_j . We illustrate this with the following examples.

Example 1 (Repeat Codes with BECs) Consider the model of Fig. 2 with a length- n repeat code. Suppose the communication and extrinsic channels are BECs with erasure probabilities q and p , respectively. We thus have $I_A = I(V_1; A_1) = 1 - p$. Furthermore, for the case $\underline{v} = \underline{x}$ we have

$$\begin{aligned} I_E &= \frac{1}{n} \sum_{j=1}^n I(X_j; \underline{Y} \underline{A}_{[j]}) \\ &= H(X_1) - H(X_1 | \underline{Y} \underline{A}_{[1]}) \\ &= 1 - q^n p^{n-1}, \end{aligned} \quad (14)$$

where the second step follows by the symmetry of the code. We plot I_E versus I_A in Fig. 4 where we have chosen $q = 0.9$ and $n = 2, 3, 4$. Observe that the repeat codes perform best at low values of I_A in the sense that the slopes of the curves are large there.

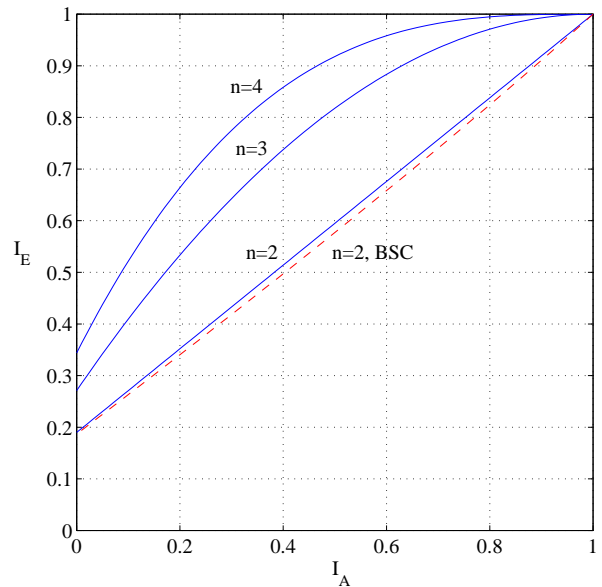


Fig. 4: EXIT functions for repeat codes of length $n = 2, 3, 4$. The communication and extrinsic channels are either both BECs (solid lines) or both BSCs (dashed line).

Example 2 (Repeat Codes with BSCs) Consider again Fig. 2. Suppose we have a length-2 repeat code, and that the communication and extrinsic channels are binary symmetric channels (BSCs) with crossover probabilities ϵ and δ , respectively. We now have $I_A = I(V_1; A_1) = 1 - h(\delta)$ where $h(x) = -x \log_2(x) - (1-x) \log_2(1-x)$ is the binary entropy function. For the case $\underline{v} = \underline{x}$ we use (11) to compute

$$\begin{aligned} I_E &= 1 - \left\{ [(1-\epsilon)^2(1-\delta) + \epsilon^2\delta] h\left(\frac{\epsilon^2\delta}{(1-\epsilon)^2(1-\delta) + \epsilon^2\delta}\right) \right. \\ &\quad + [(1-\epsilon)^2\delta + \epsilon^2(1-\delta)] h\left(\frac{\epsilon^2(1-\delta)}{(1-\epsilon)^2\delta + \epsilon^2(1-\delta)}\right) \\ &\quad \left. + 2\epsilon(1-\epsilon)h(\delta) \right\}. \end{aligned} \quad (15)$$

We plot I_E versus I_A in Fig. 4 where we have chosen $\epsilon = 0.316$. This choice makes the capacity of the BSC with output \underline{y} approximately the same as the capacity of the BEC of Example 1, i.e., $C = 1 - h(0.316) \approx 0.1$. Observe that the BSC curve is quite close to the BEC curve but lies below it.

Example 3 (Parity-check Codes with BECs) Consider once again Fig. 2 and suppose the code is a parity-check code. For the case $\underline{v} = \underline{x}$ we have

$$\begin{aligned} I_E &= \frac{1}{n} \sum_{j=1}^n I(X_j; \underline{Y} \underline{A}_{[j]}) \\ &= H(X_1) - H(X_1 | \underline{Y} \underline{A}_{[1]}) \\ &= 1 - [1 - (1-q) - q(1-qp)^{n-1}] \\ &= (1-q) + q(1-qp)^{n-1}. \end{aligned} \quad (16)$$

The EXIT functions for (16) with $q = 1$ and $n = 2, 3, 4$ are plotted in Fig. 5, where $I_A = 1 - p$. Observe that the parity-check codes perform poorly at low I_A , but progressively better as I_A increases.

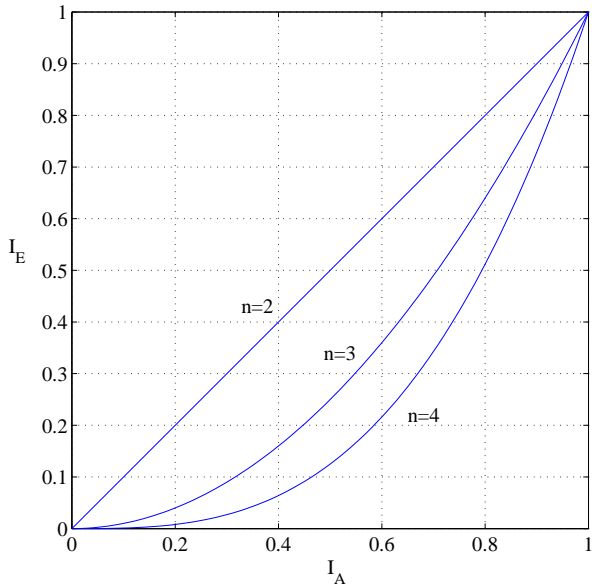


Fig. 5: EXIT functions for parity-check codes of length $n = 2, 3, 4$. The communication and extrinsic channels are both BECs, but the former channel gives no information as $q = 1$.

Example 4 (LDPC Variable Nodes with BECs)

Consider the variable nodes of an LDPC code and suppose they have degree d_v . In a factor graph [8] these nodes have one edge connected to a channel output and d_v edges connected to the interleaver. We can thus use the model of Fig. 3 with $\underline{u} = \underline{x}$ being one bit, and Encoder 2 a length- d_v repeat code. We again make the communication and extrinsic channels BECs with erasure probabilities q and p , respectively. We compute (11) as

$$I_E = 1 - qp^{d_v-1}, \quad (17)$$

or $I_E(I_A) = 1 - q(1 - I_A)^{d_v-1}$. Fig. 1 shows two examples of such curves when $d_v = 2$ and $q = 0.3, 0.5$.

Example 5 (LDPC Check Nodes with a BEC)

Consider the check nodes of an LDPC code and suppose they have degree d_c . We use the model of Fig. 3 with $\underline{y} = \underline{0}$ and with Encoder 2 a length- d_c parity-check code. Let the extrinsic channel be a BEC with erasure probability p so (11) simplifies to

$$I_E = (1 - p)^{d_c-1}. \quad (18)$$

Thus, the EXIT curve is $I_E(I_A) = (I_A)^{d_c-1}$. An example of such a curve with $d_c = 4$ is plotted in Fig. 1.

C. MIXTURES OF CODES

Suppose we encode the information vector \underline{u} by splitting it into several vectors $\underline{u}_1, \underline{u}_2, \dots, \underline{u}_{n_u}$, and then encoding each of these separately. Let \underline{v}_i and \underline{e}_i , $i = 1, \dots, n_u$, be those portions of the respective \underline{v} and \underline{e} corresponding to \underline{u}_i . Denote the length of \underline{v}_i by ℓ_i . Equation (8) then simplifies to

$$\begin{aligned} I_E &= \sum_{i=1}^{n_u} \frac{\ell_i}{m} \left[\frac{1}{\ell_i} \sum_{j=1}^{\ell_i} I(V_{ij}; E_{ij}) \right] \\ &= \sum_{i=1}^{n_u} \gamma_i I_{E_i}, \end{aligned} \quad (19)$$

where V_{ij} and E_{ij} are the j th entries of \underline{V}_i and \underline{E}_i , respectively, $\gamma_i = \ell_i/m$ and $I_{E_i} = (1/\ell_i) \sum_{j=1}^{\ell_i} I(V_{ij}; E_{ij})$. Observe that I_{E_i} is simply the average extrinsic information for the i th component code. Thus, the EXIT function I_E is the average of the component EXIT functions I_{E_i} .

Example 6 (Irregular LDPC Codes with BECs) An irregular LDPC code [4] can be viewed as having a mixture of repeat-codes on the left and a mixture of parity-check codes on the right. For example, suppose half of the variable nodes have degree 2 and the other half have degree 3. Because (8) is an average over the edges, and not the nodes, we first compute that 40% and 60% of the edges are connected to degree-2 and degree-3 variable nodes, respectively. Thus, using Example 4 we find that (19) simplifies to

$$I_E = 1 - q(0.4p + 0.6p^2), \quad (20)$$

where $\gamma_1 = 0.4$ and $\gamma_2 = 0.6$. The γ_i are here the same as the left degree sequence coefficients λ_{i+1} of [4]. One can similarly derive the EXIT function for a mixture of check nodes.

III. ERASURE CHANNEL EXIT PROPERTIES

The rest of this document is concerned with the special case where the *a priori* values \underline{w} are modeled as coming out of a BEC. We derive two kinds of properties of EXIT functions for such situations. The first concerns a relation between a linear code and its dual, and the second relates the area under an EXIT function to the code rate.

A. DUALITY PROPERTY

The following theorem can be proved by using combinatorial arguments.

Theorem 1 Consider Fig. 2 and suppose $\underline{y} = \underline{0}$ and the extrinsic channel is a binary erasure channel. Then the EXIT function $I_E(\cdot)$ of a linear code and its dual are related as follows

$$I_E^\perp(I_A) = 1 - I_E(1 - I_A), \quad (21)$$

where $I_E^\perp(\cdot)$ is the EXIT function of the dual code and $I_A = 1 - p$.

This theorem can be generalized to the case where the communication channel is a BEC. As an example, consider the repeat code curve $1 - q^n p^{n-1}$ in (14). Setting $q = 1$ we obtain $I_E(1 - p) = 1 - p^{n-1}$. The dual code is the parity check code which according to (16) has $I_E^\perp(1 - p) = (1 - p)^{n-1}$ for $q = 1$. But this is the same as $1 - I_E(p)$, as required by Theorem 1.

B. AREA PROPERTY

The following theorem can be proved by using the information theoretic identity derived in [9]. Let $\mathcal{A} = \int_0^1 I_E(I_A) dI_A$ be the area under the EXIT function.

Theorem 2 Consider Fig. 3 and the extrinsic information (11). For any codes (linear or not) and any communication channel (memoryless or not) we have

$$\mathcal{A} = \frac{1}{m} \left(\sum_{j=1}^m H(V_j) \right) - \frac{1}{m} H(\underline{V}|\underline{Y}) \quad (22)$$

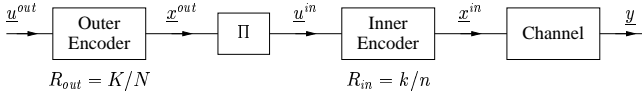


Fig. 6: Serially concatenated encoder.

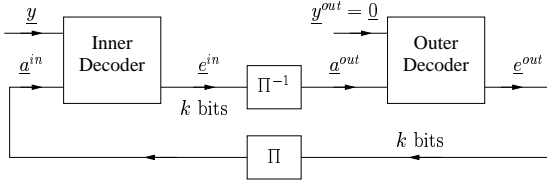


Fig. 7: An iterative decoder for a serially concatenated code.

if the extrinsic channel is a BEC. In particular, if Encoder 2 in Fig. 3 is a linear code whose generator matrix has no all-zeros columns, then (22) becomes

$$\mathcal{A} = 1 - \frac{1}{m} H(\underline{V}|\underline{Y}). \quad (23)$$

For example, consider the repeat code curve $1 - q^n p^{n-1}$ in (14). The area under this curve is $1 - q^n/n$. But we also have $m = n$ and $H(\underline{V}|\underline{Y}) = H(\underline{X}|\underline{Y}) = q^n$, so (23) gives the desired result. The impact of Theorem 2 is that it restricts the form of the EXIT function. Moreover, one can often directly relate \mathcal{A} to the rate of the code, as shown next.

IV. EXIT FOR SERIALLY CONCATENATED CODES

A serially concatenated code [10] has an $[N, K]$ outer code, meaning the outer code has 2^K code words of length N , and an $[n, k]$ inner code with $k = N$ (see Fig. 6). The K information bits \underline{u}^{out} , are mapped by the outer encoder to N coded bits \underline{x}^{out} . An interleaver permutes the bits in \underline{x}^{out} to \underline{u}^{in} and the inner encoder maps \underline{u}^{in} to the length- n vector \underline{y}^{in} . Thus, the overall rate of the code is $R = R_{out}R_{in} = K/n$ where $R_{out} = K/N = K/k$ and $R_{in} = k/n$. We consider only the case where both codes are linear.

The iterative decoder for the serially concatenated code is shown in Fig. 7. Consider first the outer decoder for which we use the model of Fig. 2 with $\underline{v} = \underline{x} = \underline{x}^{out}$ and $\underline{y} = \underline{0}$. Theorem 2 tells us that for a BEC the area under the outer code curve I_E^{out} is, using $m = N$ and $H(\underline{V}) = K$,

$$\mathcal{A}_{out} = 1 - K/N = 1 - R_{out}. \quad (24)$$

Next, for the inner decoder we set $\underline{v} = \underline{u} = \underline{u}^{in}$. Theorem 2 now tells us that the area under the inner code curve I_E^{in} is, using $m = k = H(\underline{X})$ and $H(\underline{V}|\underline{Y}) = H(\underline{X}|\underline{Y})$,

$$\mathcal{A}_{in} = I(\underline{X}; \underline{Y})/k = [I(\underline{X}; \underline{Y})/n]/R_{in}. \quad (25)$$

Equations (24) and (25) have the following implications. Recall that for iterative decoding to be successful we require the outer code curve to lie above the inner code curve. For serially concatenated codes this means one must have $1 - \mathcal{A}_{out} < \mathcal{A}_{in}$, where \mathcal{A}_{out} and \mathcal{A}_{in} are the respective areas under the outer and inner EXIT functions. This area inequality can be rewritten as $R_{out} < I(\underline{X}; \underline{Y})/k$ or

$$R_{out}R_{in} < I(\underline{X}; \underline{Y})/n \leq C, \quad (26)$$

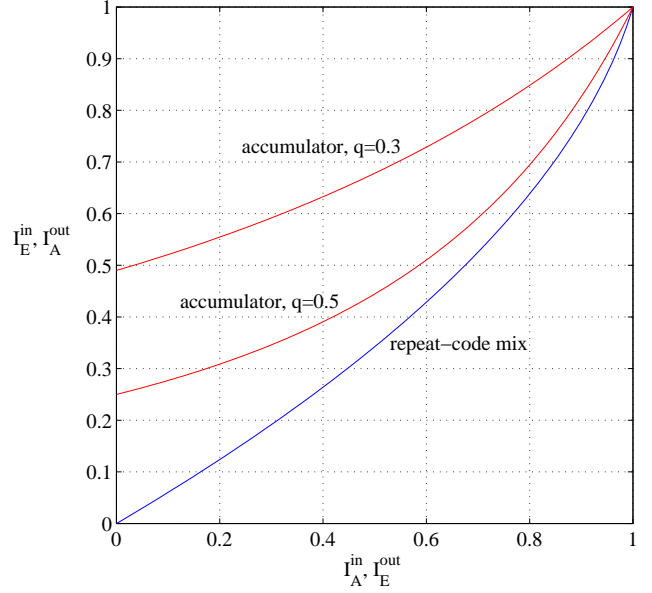


Fig. 8: EXIT functions for a repeat-accumulate code on the BEC with erasure probabilities $q = 0.3$ and $q = 0.5$.

where C is the capacity of the communication channel. Thus, we get the satisfying, if not surprising, result that the overall rate must be less than capacity for successful decoding [11]. However, the bound (26) says much more because $I(\underline{X}; \underline{Y})/n$ equals capacity only if the inner code has rate one. Thus, any inner code with $R_{in} < 1$ has an inherent capacity loss which the outer code cannot recover. This suggests that for serially concatenated codes it is a good idea to use a rate-one inner code when iteratively decoding (see, e.g., [12, Sec. III]). We consider such an example next.

Example 7 (Repeat-accumulate Codes with BECs)

A repeat-accumulate code [13] has an accumulator as the inner code and a mixture of repeat-codes as the outer code. The EXIT function of the accumulator is (see [14])

$$I_E^{in} = \left[\frac{1-q}{1-q I_A^{in}} \right]^2, \quad (27)$$

where $I_A^{in} = 1 - p$. This code has $R_{in} = 1$ and $I(\underline{X}; \underline{Y})/n = 1 - q$ for all n . It is easy to check that the area under the curve (27) is precisely $C = 1 - q$. For the outer code we connect 40% of the edges to degree-2 variable nodes and 60% of the edges to degree-3 variable nodes. We thus have $R_{out} = 0.4$ and, using (14) and (19),

$$I_E^{out} = 1 - 0.4p - 0.6p^2. \quad (28)$$

The area under the curve is precisely $1 - R_{out} = 0.6$.

The EXIT chart is plotted in Fig. 8 for erasure probabilities $q = 0.3$ and $q = 0.5$. Observe that for both of these q the decoder's per-edge erasure probability can be made to approach zero. The threshold for this code is in fact $q = 5/9$ for which the capacity is $C = 4/9 \approx 0.4444$. Thus, these repeat-accumulate codes do not approach capacity. We remark that a more general class of repeat-accumulate codes can approach capacity on a BEC [14].

As a final note, observe that for a rate-one code the area difference $\mathcal{A}_{in} - (1 - \mathcal{A}_{out})$ is exactly $C - R$. In other words,

the area between the curves corresponds exactly to the rate “loss”. This means that to approach capacity one must *match the outer code curve exactly to the inner code curve*. Furthermore, the smaller the area between the curves the larger the number of iterations that are needed to achieve a desired per-edge erasure probability. The EXIT chart thus shows graphically how the decoding complexity (in terms of the number of iterations) increases as one approaches capacity.

V. EXIT FOR LDPC CODES

As we have seen in Examples 4, 5 and 6, equation (11) applies to both regular and irregular LDPC codes. Our aim in this section is to relate the area under the LDPC curves to the code rate in a way analogous to (24) and (25). Observe that the design rate R of the code is determined by the number of variable nodes n_v and the number of check nodes n_c via

$$R = (n_v - n_c)/n_v = 1 - n_c/n_v. \quad (29)$$

Let d_v and d_c be the *average* degree of the variable and check nodes, respectively. Thus the number of edges is both $n_v d_v$ and $n_c d_c$, giving

$$R = 1 - d_v/d_c. \quad (30)$$

Furthermore, for the areas \mathcal{A}_v and \mathcal{A}_c under the respective variable and check node curves we use Theorem 2 to compute

$$\mathcal{A}_v = 1 - \frac{n_v q}{n_v d_v} = 1 - \frac{1 - C}{d_v}, \quad (31)$$

$$\mathcal{A}_c = 1 - \frac{n_c(d_c - 1)}{n_c d_c} = \frac{1}{d_c}, \quad (32)$$

where $H(\underline{V}|\underline{Y}) = H(\underline{X}|\underline{Y}) = n_v q$ for the variable nodes and $H(\underline{V}|\underline{Y}) = H(\underline{V}) = n_c(d_c - 1)$ for the check nodes. From (31) and (32) we obtain the following relation between the EXIT areas and the rate of the code:

$$\frac{1 - \mathcal{A}_v}{\mathcal{A}_c} = \frac{1 - C}{1 - R}. \quad (33)$$

Equation (33) has the following implications. For the decoding to be successful we require the variable node curve to lie above the check node curve. This means $1 - \mathcal{A}_v < \mathcal{A}_c$, which is possible only if $R < C$. Furthermore, any area gap between the two curves translates into a rate “loss”, except now this loss is not given by a difference in areas as for serially concatenated codes, but by equation (33). Thus we have the result that to approach capacity one must *match the variable node curve exactly to the check node curve* (see also [15, 16, 17]).

REFERENCES

- [1] S. ten Brink, “Convergence of iterative decoding,” *Electron. Lett.*, vol. 35, no. 10, pp. 806–808, May 1999.
- [2] R.G. Gallager, “Low density parity check codes,” Sc.D. thesis, Sept. 1960.
- [3] R.G. Gallager, “Low-density parity-check codes,” *IRE Trans. Inform. Theory*, vol. 8, pp. 21–28, Jan. 1962.
- [4] M.G. Luby, M. Mitzenmacher, M.A. Shokrollahi, and D.A. Spielman, “Efficient erasure correcting codes,” *IEEE Trans. Inform. Theory*, vol. 47, no. 2, pp. 569–584, Feb. 2001.
- [5] T.J. Richardson and R.L. Urbanke, “The capacity of low-density parity-check codes under message-passing decoding,” *IEEE Trans. Inform. Theory*, vol. 47, no. 2, pp. 599–618, Feb. 2001.
- [6] J. Hagenauer, E. Offer, and L. Papke, “Iterative decoding of binary block and convolutional codes,” *IEEE Trans. Inform. Theory*, vol. 42, no. 2, pp. 429–445, March 1996.
- [7] L. Bahl, J. Cocke, F. Jelinek, and J. Raviv, “Optimal decoding of linear codes for minimizing symbol error rate,” *IEEE Trans. Inform. Theory*, vol. 20, pp. 284–287, March 1974.
- [8] F.R. Kschischang, B.J. Frey, and H.-A. Loeliger, “Factor graphs and the sum-product algorithm,” *IEEE Trans. Inform. Theory*, vol. 47, no. 2, pp. 498–519, Feb. 2001.
- [9] S. ten Brink, “Exploiting the chain rule of mutual information for the design of iterative decoding schemes,” in *Proc. 39th Ann. Allerton Conf. on Commun., Control, and Computing*, Monticello, Urbana-Champaign, Ill., USA, Oct. 2001.
- [10] S. Benedetto, D. Divsalar, G. Montorsi, and F. Pollara, “Serial concatenation of interleaved codes: performance analysis, design, and iterative decoding,” *IEEE Trans. Inform. Theory*, vol. 44, no. 3, pp. 909–926, May 1998.
- [11] C.E. Shannon, “A mathematical theory of communication,” *Bell Syst. Tech. J.*, vol. 27, pp. 379–423 and 623–656, July and October 1948, Reprinted in *Claude Elwood Shannon: Collected Papers*, pp. 5–83, (N.J.A. Sloane and A.D. Wyner, eds.) Piscataway: IEEE Press, 1993.
- [12] S. ten Brink, “Code doping for triggering iterative decoding convergence,” in *Proc. 2001 IEEE Int. Symp. Inform. Theory*, Washington, D.C., USA, June 2001, p. 235.
- [13] D. Divsalar, H. Jin, and R.J. McEliece, “Coding theorems for ‘turbo-like’ codes,” in *Proc. 36th Allerton Conf. on Comm., Control, Comp.*, Allerton, Illinois, USA, Sept. 1998, pp. 201–210.
- [14] H. Jin, A. Khandekar, and R. McEliece, “Irregular repeat-accumulate codes,” in *Proc. 2nd Int. Conf. Turbo Codes*, Brest, France, Sept. 2000.
- [15] M.A. Shokrollahi, “New sequences of linear time erasure codes approaching the channel capacity,” in *Proc. 13th Conf. Applied Algebra, Error Correcting Codes, and Cryptography (Lecture Notes in Computer Science)*, Berlin, Germany, 1999, pp. 65–76, Springer Verlag.
- [16] T.J. Richardson and R.L. Urbanke, “Design of capacity-approaching irregular low-density parity-check codes,” *IEEE Trans. Inform. Theory*, vol. 47, no. 2, pp. 619–637, Feb. 2001.
- [17] P. Oswald and A. Shokrollahi, “Capacity-achieving sequences for the erasure channel,” in *Proc. 2001 IEEE Int. Symp. Inform. Theory*, Washington, D.C., USA, June 2001, p. 48.